# Implementation of the Low-Noise, 3-D Ray-Trace Inverse-Projection Method in the Radiation-Hydrodynamics Code *HYDRA*

Omega 60-beam;
- ~25M rays/ray-trace cycle
- Tail end of pulse; $t \sim 2.3$ ns
- CR ~ 430/145 = 3

Random rays

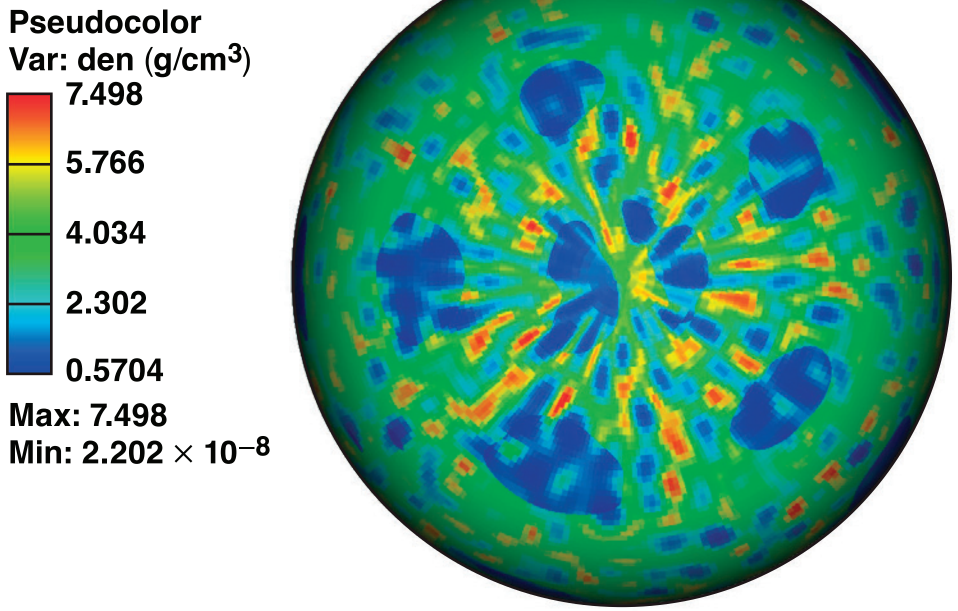


Inverse projection

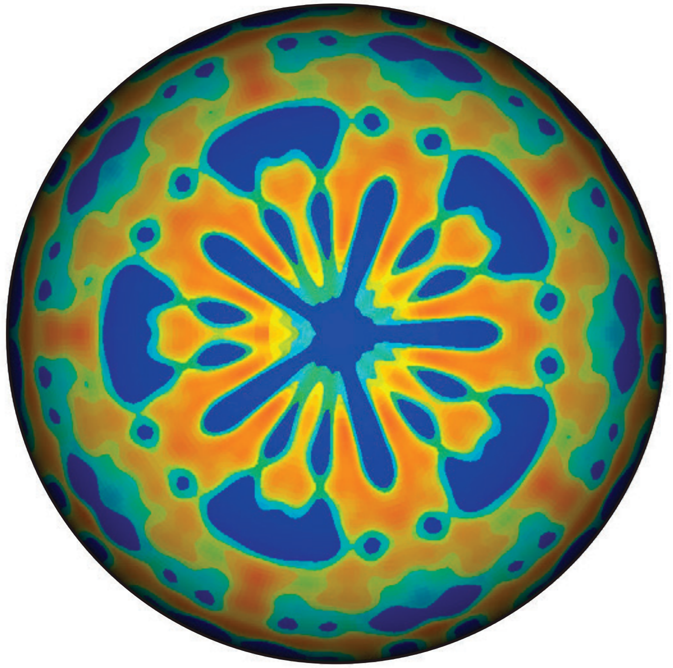

(Polar view; constant radius)

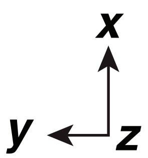



J. A. Marozas
University of Rochester
Laboratory for Laser Energetics



60th Annual Meeting of the American Physical Society Division of Plasma Physics
Portland, OR
5–9 November 2018

Summary

# Significant progress has been made implementing the LLE ray trace in *HYDRA*;* however, further work remains to minimize numerical noise

- The complete inverse projection method implemented in *DRACO*** offers many advantages that can port to *HYDRA*
  - low ray density achieves low noise levels; includes additional methods (below)
  - smooth deposition maximizes time steps → faster execution
  - the anticipated smooth deposition exposes potential noise sources
- The first stage of implementation is complete and significantly reduced noise levels to the order of the overlapped nonuniformity (~ few %)
- Additional methods are required for high-fidelity (noise below overlapped nonuniformity) direct-drive simulations
  - random dithering
  - dynamic refraction compensation (multiple methods)
  - adaptive ray integrators and cell-edge detection

- **Work on adapting the existing CBET model to direct drive in *HYDRA* will follow.**

*M. M. Marinak *et al.*, Phys. Plasmas 8, 2275 (2001).
**J. A. Marozas *et al.*, Phys. Plasmas 25, 056314 (2018).
M. M. Marinak *et al.*, UP11.00115, this conference.

TC14592

# Collaborators

**G. D. Kerbel, M. M. Marinak, and S. Sepke**

Lawrence Livermore National Laboratory

# Four main categories of reducing laser deposition noise are included in the LLE* ray trace; staged approach

Phase 1

- Ray-trace noise reduction
  - an inverse-projection algorithm defines the initial ray-position distribution and energies—complete
    - this is the primary noise-reduction aspect

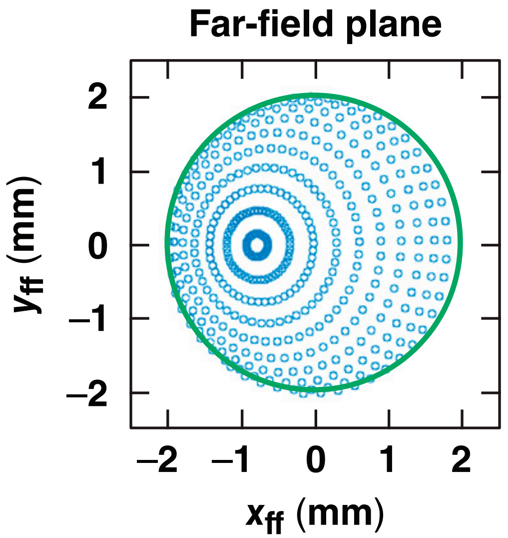


Inverse projection

TC7537d

*J. A. Marozas *et al.*, Phys. Plasmas 25, 056314 (2018).

# Four main categories of reducing laser deposition noise are included in the LLE* ray trace; staged approach

Phase 1

Phase 2

- Ray-trace noise reduction
  - an inverse-projection algorithm defines the initial ray-position distribution and energies—complete
    - this is the primary noise-reduction aspect
  - dynamic adjustment of inverse projection partially compensates for refraction and reduces noise
    - in progress

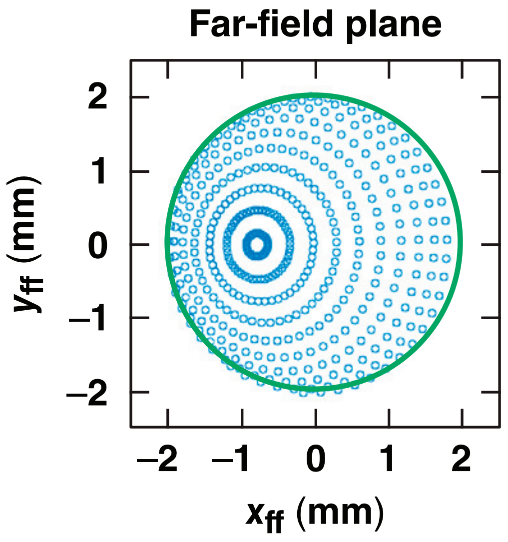


Inverse projection

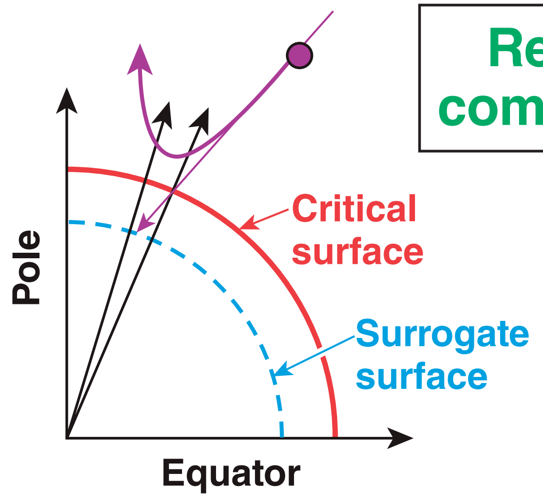


Refraction compensation

TC7537e

*J. A. Marozas *et al.*, Phys. Plasmas 25, 056314 (2018).

# Four main categories of reducing laser deposition noise are included in the LLE* ray trace; staged approach

UR LLE

Phase 1

Phase 2

Phase 3

Phase 4

- Ray-trace noise reduction
  - an inverse-projection algorithm defines the initial ray-position distribution and energies—complete
    - this is the primary noise-reduction aspect
  - dynamic adjustment of inverse projection partially compensates for refraction and reduces noise
    - in progress
  - adaptive integrators
    - future work
  - accurate cell-edge crossing detection using root polishing; never loses a ray on entry/exit
    - future work

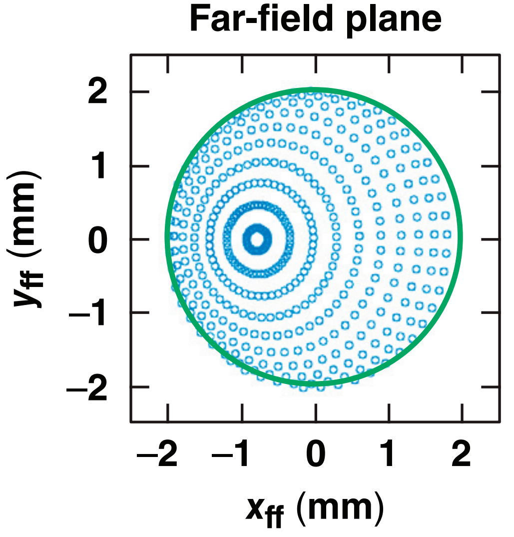


Inverse projection

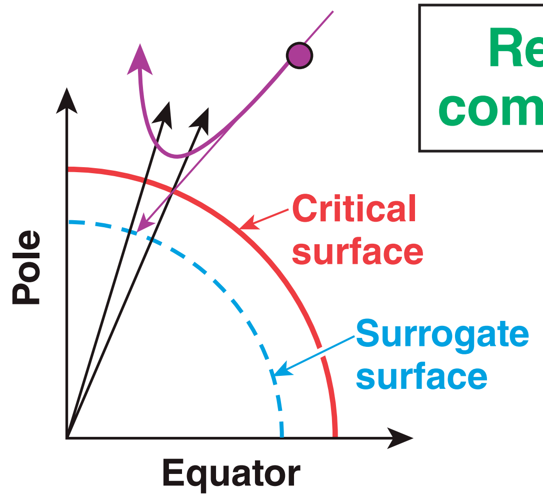


Refraction compensation

TC7537f

*J. A. Marozas *et al.*, Phys. Plasmas 25, 056314 (2018).

# Four main categories of reducing laser deposition noise are included in the LLE* ray trace; staged approach



Phase 1

Phase 2

Phase 3

Phase 4

- Ray-trace noise reduction
  - an inverse-projection algorithm defines the initial ray-position distribution and energies—complete
    - this is the primary noise-reduction aspect
  - dynamic adjustment of inverse projection partially compensates for refraction and reduces noise
    - in progress
  - adaptive integrators
    - future work
  - accurate cell-edge crossing detection using root polishing; never loses a ray on entry/exit
    - future work
- Applying higher ray density and boxcar filtering helps reduce noise but masks any artifacts and adds diffusion

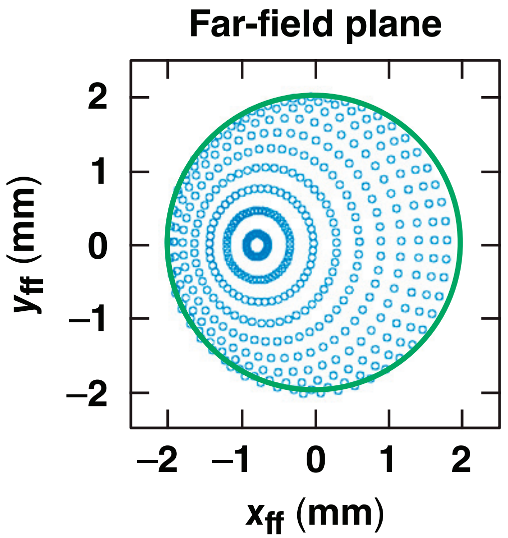


Inverse projection

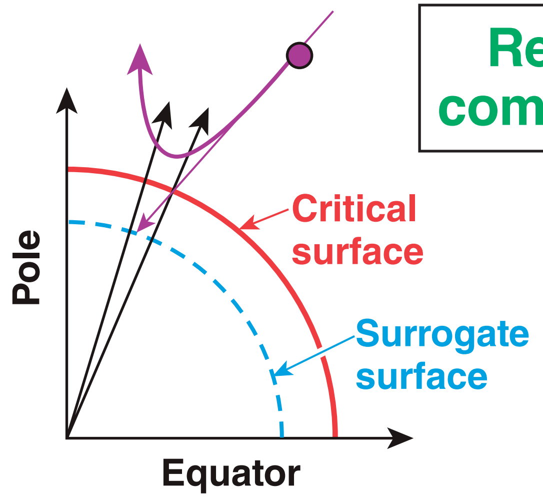


Refraction compensation

TC7537g

*J. A. Marozas *et al.*, Phys. Plasmas 25, 056314 (2018).

Phase 1

# The basic inverse projection algorithm maps out the percent of critical surfaces to form a set of aim points in 3-D *HYDRA*

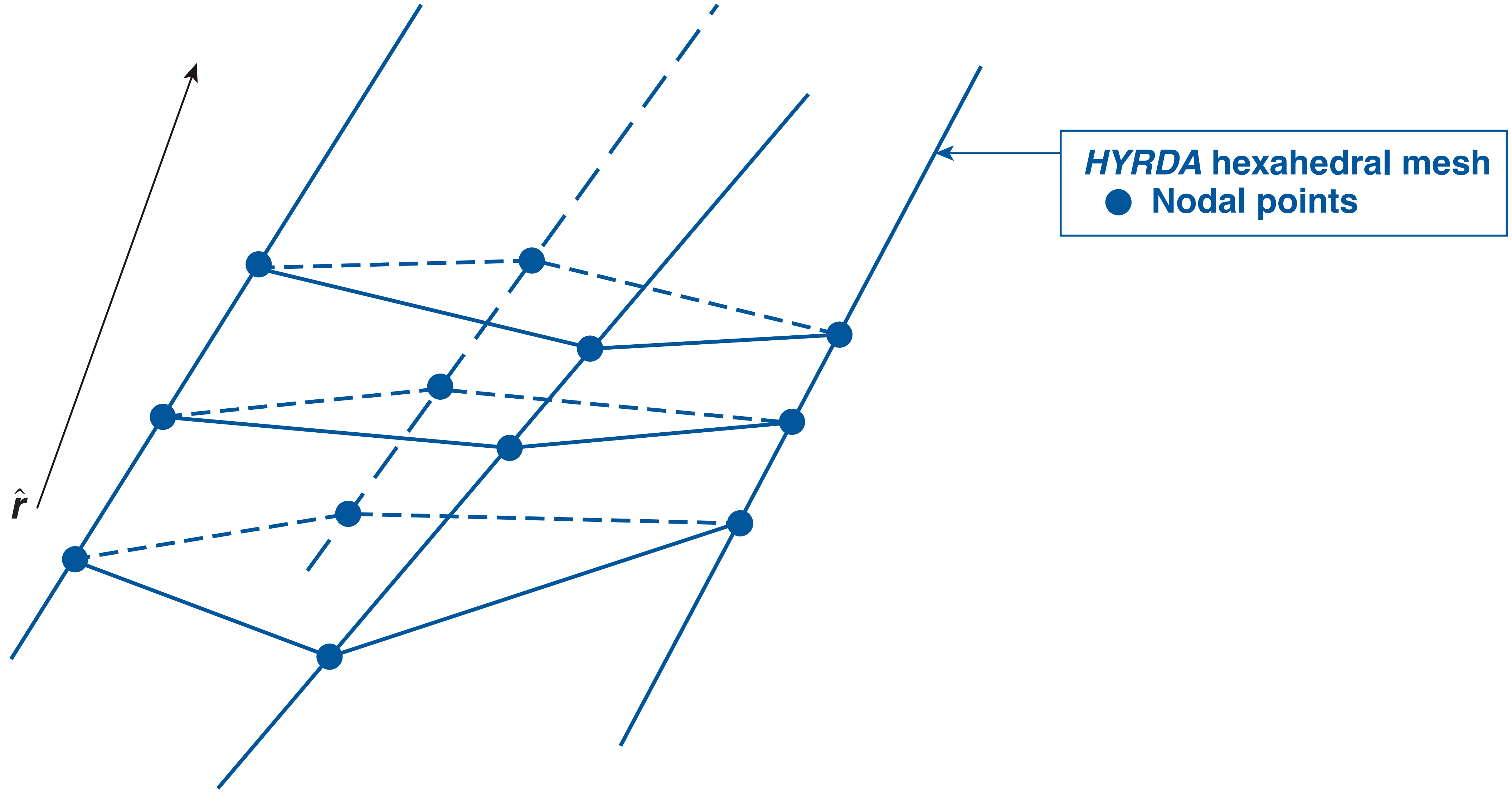


TC14505

Phase 1

# The basic inverse projection algorithm maps out the percent of critical surfaces to form a set of aim points in 3-D *HYDRA*

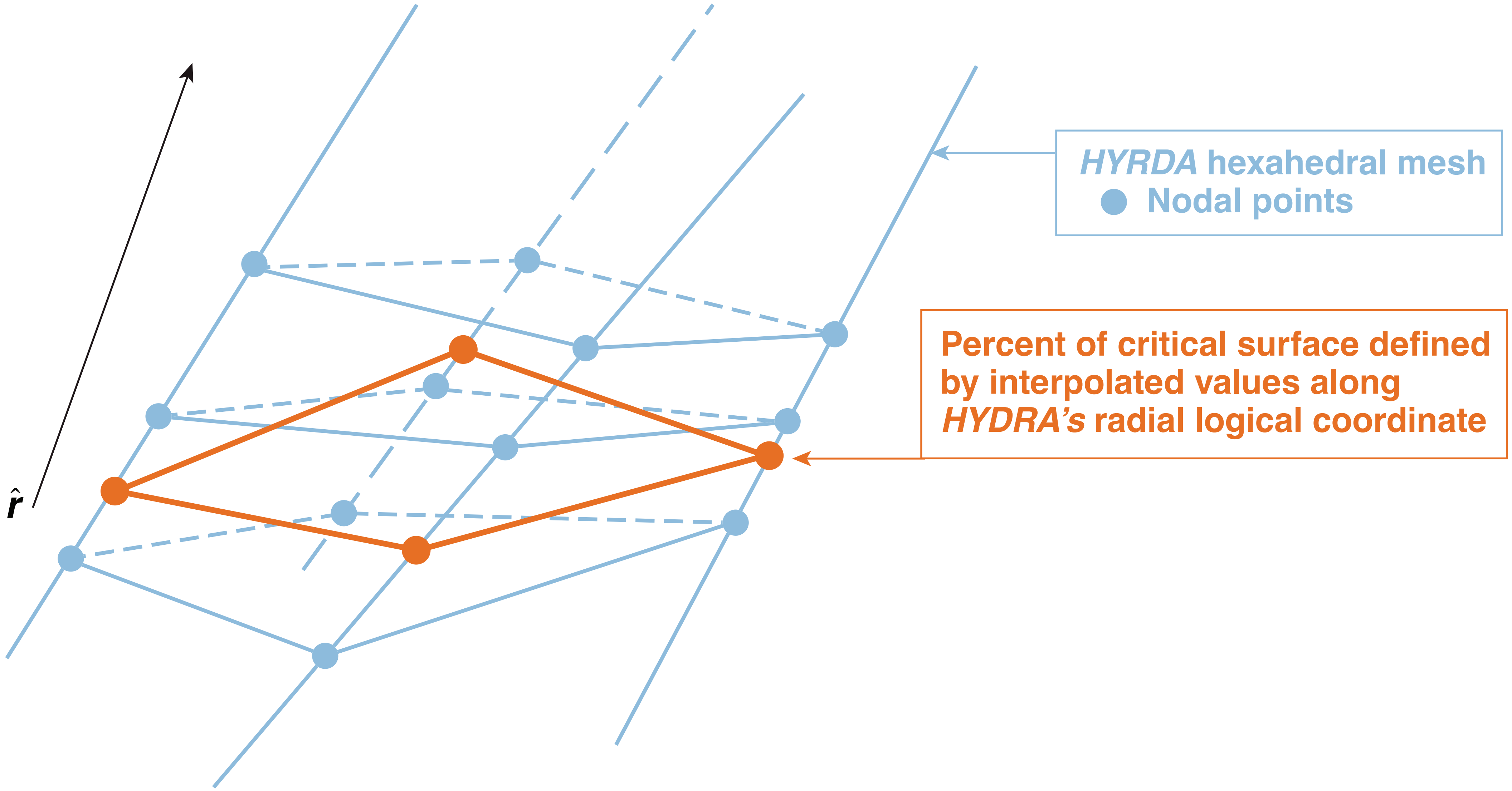


TC14505a

Phase 1

# The basic inverse projection algorithm maps out the percent of critical surfaces to form a set of aim points in 3-D *HYDRA*

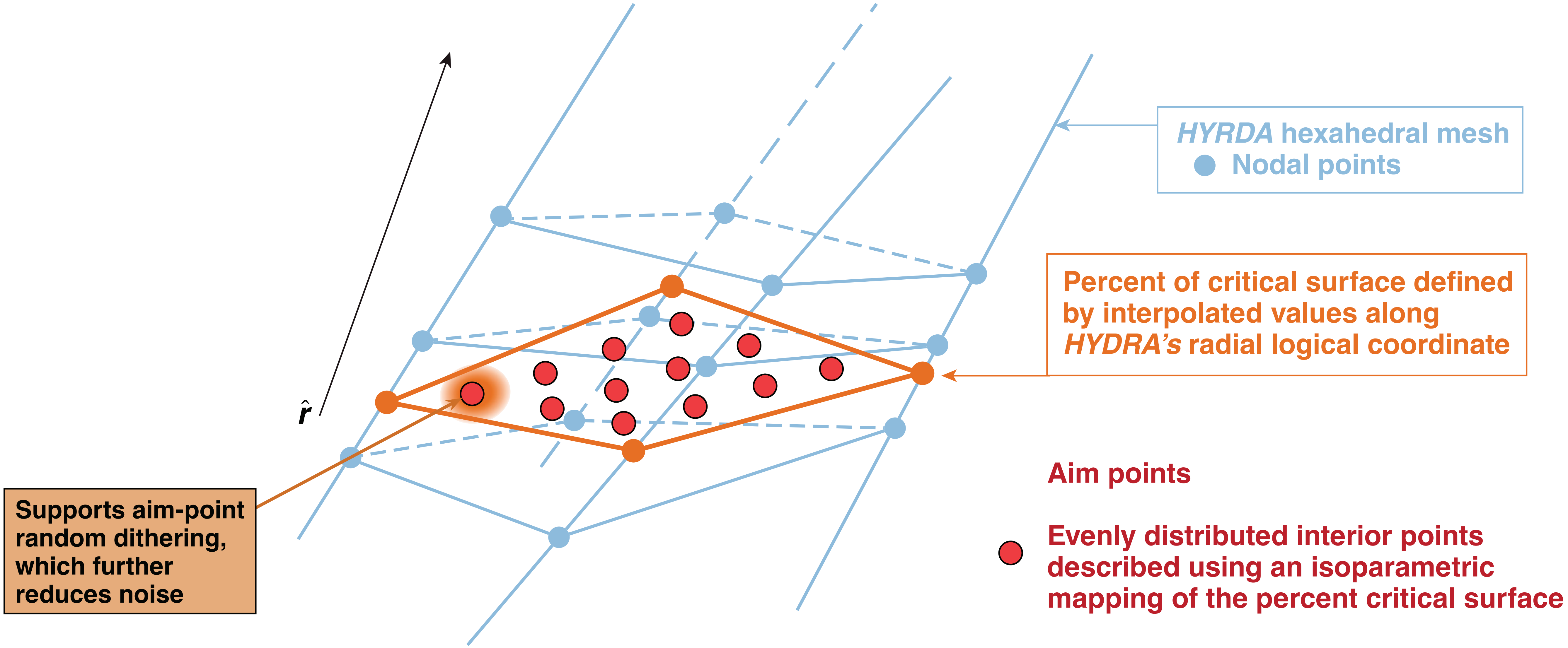


TC14505b

Phase 1

# The basic inverse-projection algorithm back-projects the aim-point distribution onto the far-field plane to form the set of launch points that do not bias the modal pattern



Rays are aimed at evenly distributed points using an isoparametric mapping within *HYDRA*'s cells

In the far-field plane, the back-projected points sample the intensity and derive energy from their area projections

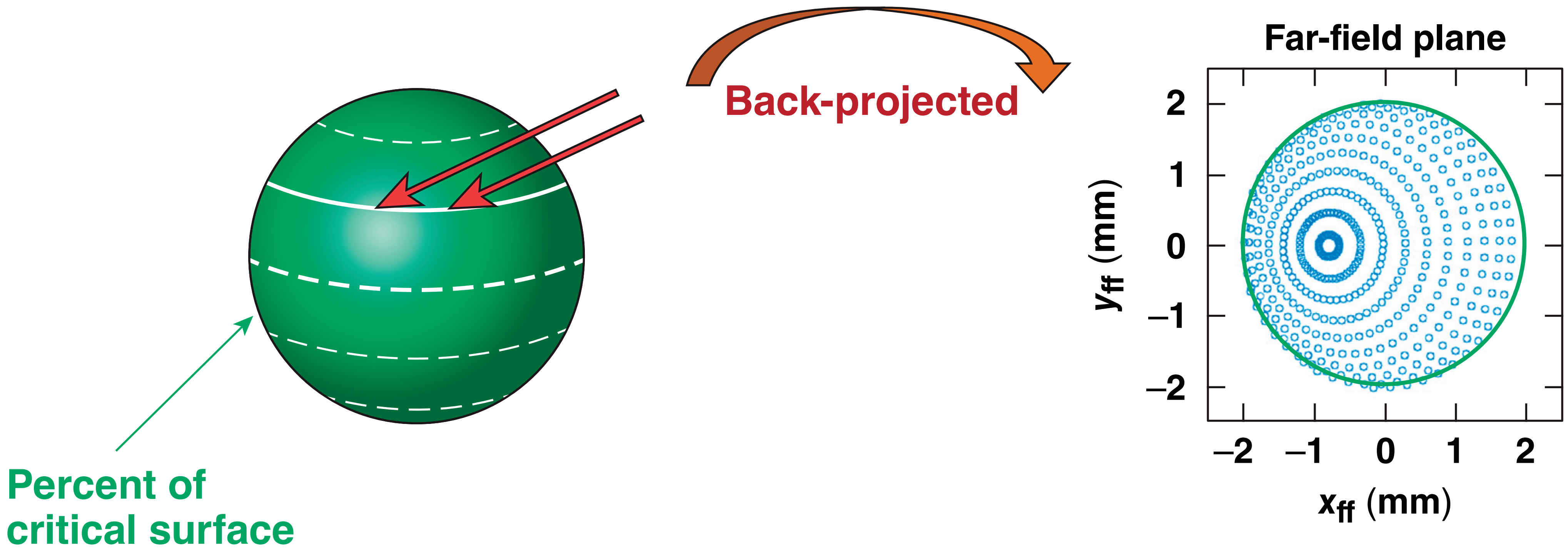


- Once the atmosphere develops, many layers of percent-critical form the surfaces

TC14594

# The early-time–deposited energy density in *HYDRA* illustrates the dramatic noise reduction—the standard illumination cf. the inverse projection methods

OMEGA 60 beam; ~4M rays
Numerical noise is most influential early in a simulation

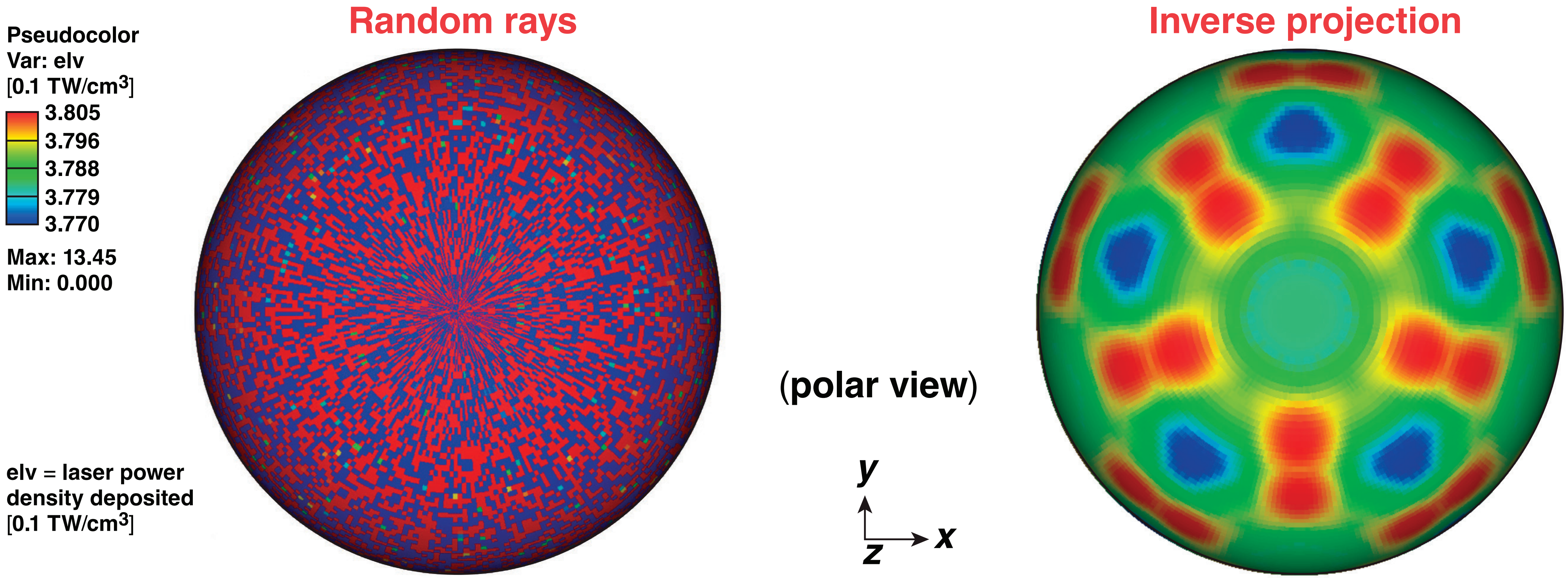


Relies on temporal averaging with staggering ray-density requirements with diminishing returns

Same ray density achieves low noise during the imprint period

TC14506

# The number of rays needs to increase > order-of-magnitude before the expected smooth pattern begins to emerge

UR LLE

**OMEGA 60 beam**
**Numerical noise is most influential early in a simulation**

Pseudocolor
Var: elv
[0.1 TW/cm$^3$]
3.805
3.796
3.788
3.779
3.770
Max: 4.684
Min: 0.000

elv = laser power density deposited [0.1 TW/cm$^3$]

**Random rays**

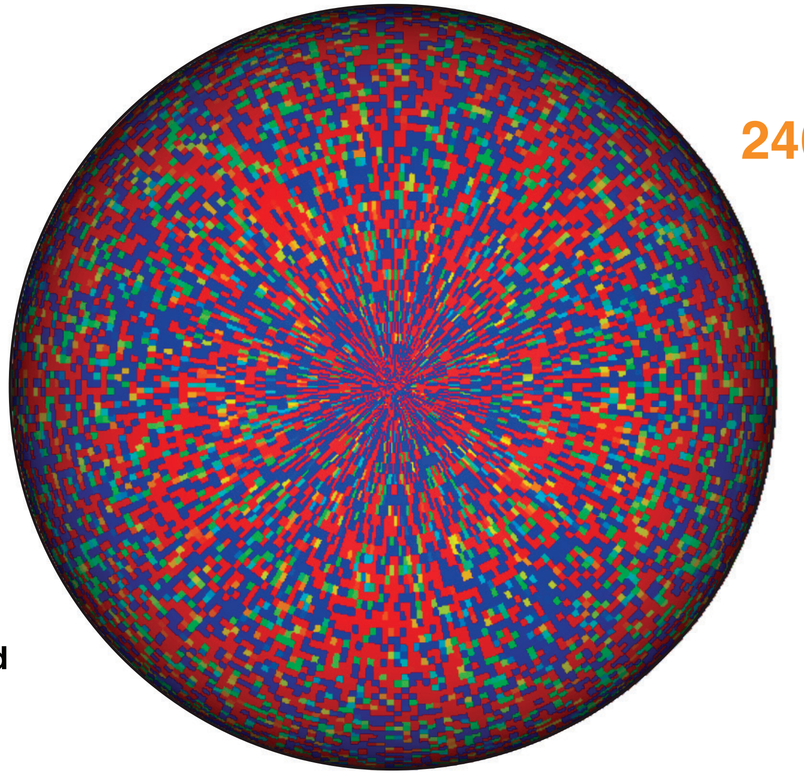

**240M rays**

Relies on temporal averaging with staggering ray-density requirements with diminishing returns

(polar view)

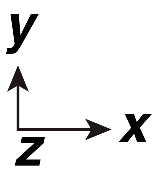


**Inverse projection**

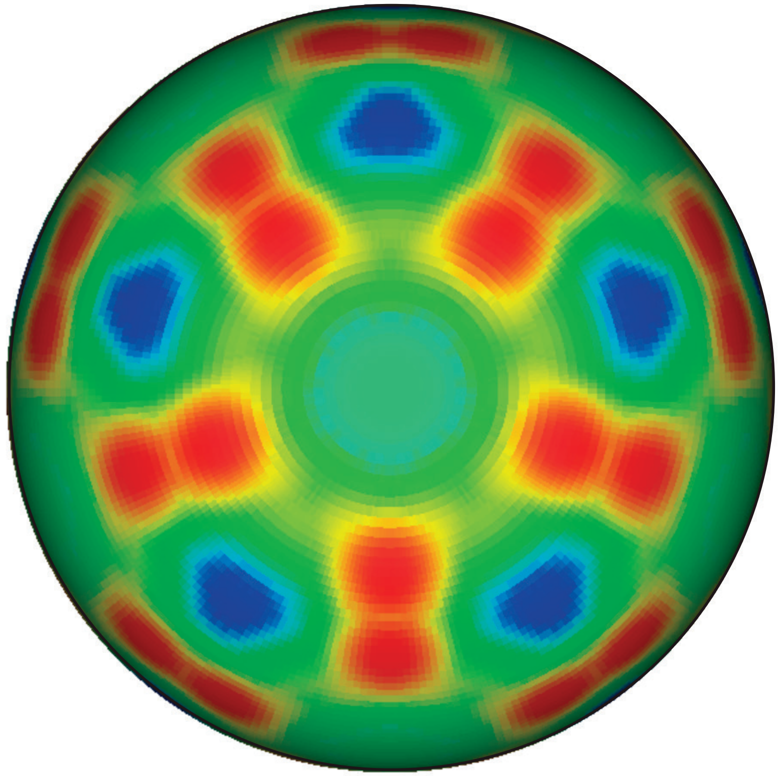

**~4M rays**

Same ray density achieves low noise during the imprint period

# The number of rays needs to increase orders of magnitude before converging towards the expected smooth pattern

**OMEGA 60 beam**
**Numerical noise is most influential early in a simulation**

Pseudocolor
Var: elv
[0.1 TW/cm3]
3.805
3.796
3.788
3.779
3.770
Max: 4.089
Min: 0.000

elv = laser power density deposited [0.1 TW/cm3]

**Random rays**

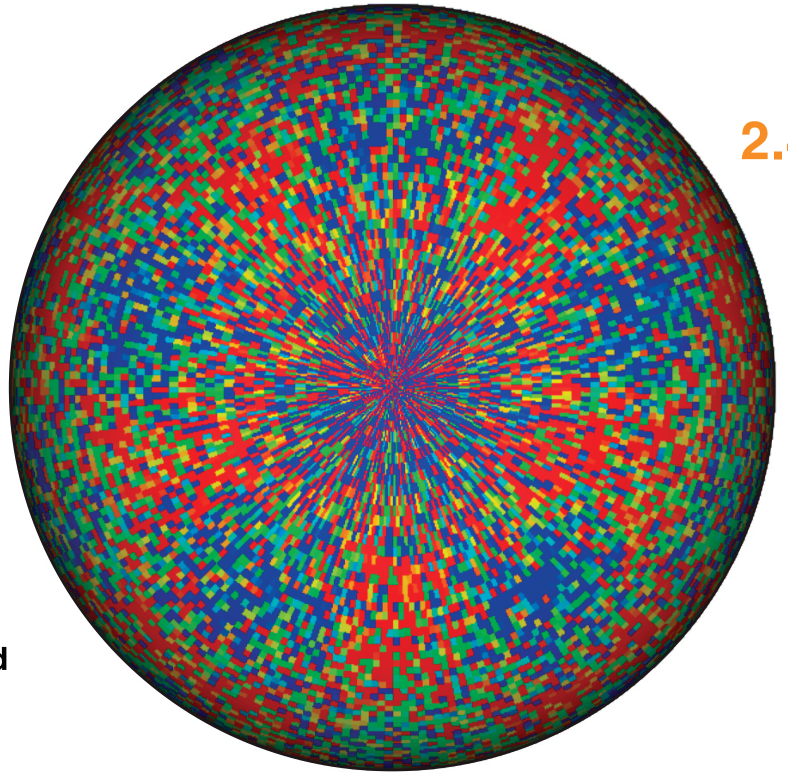

2.4G rays

(polar view)

y, x, z

**Inverse projection**

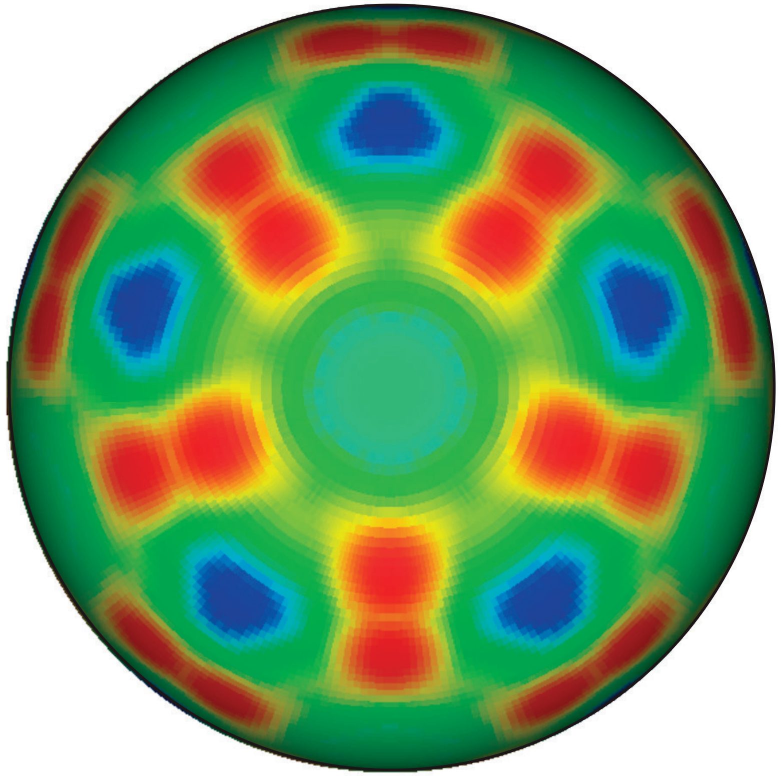

~4M rays

**Relies on temporal averaging with staggering ray-density requirements with diminishing returns**

**Same ray density achieves low noise during the imprint period**

TC14601

# The benefits of the basic inverse projection persist into late-time evolution

**OMEGA 60 beam**

- ~25M rays/ray-trace cycle
- Tail end of pulse; *t* ~ 2.3 ns
- CR ~ 430/145 = 3

**Random rays**

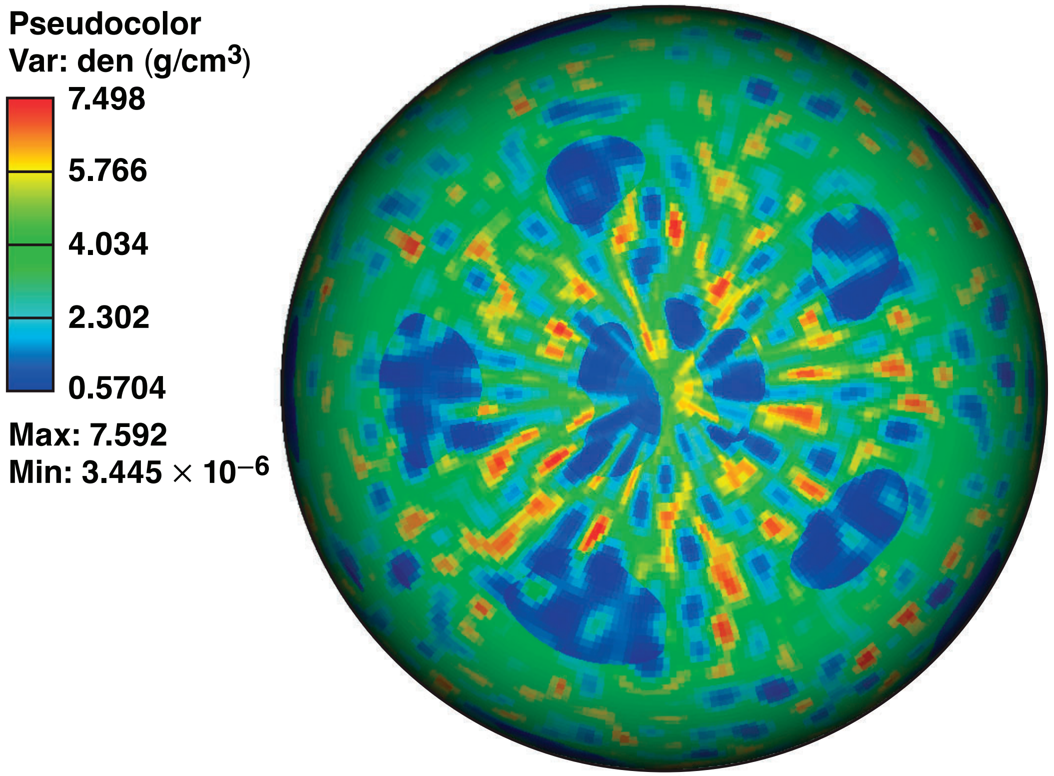


(polar view constant radius)

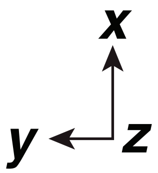


**Inverse projection**

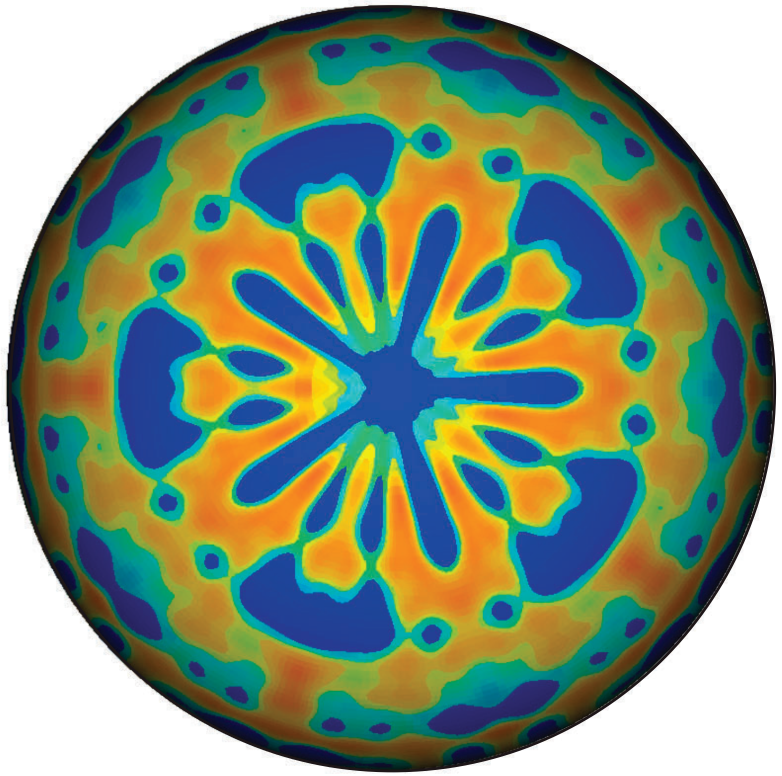

Many small high-density, random-noise features dominate the shell; the only recourse is to use many times more rays

Further improvements are necessary to eliminate the unphysical features
- Phases 2, 3, 4

TC14507

Phase 2

# A dynamic inverse-projection algorithm accounts for refraction and helps maintain smooth deposition—for example, *DRACO*

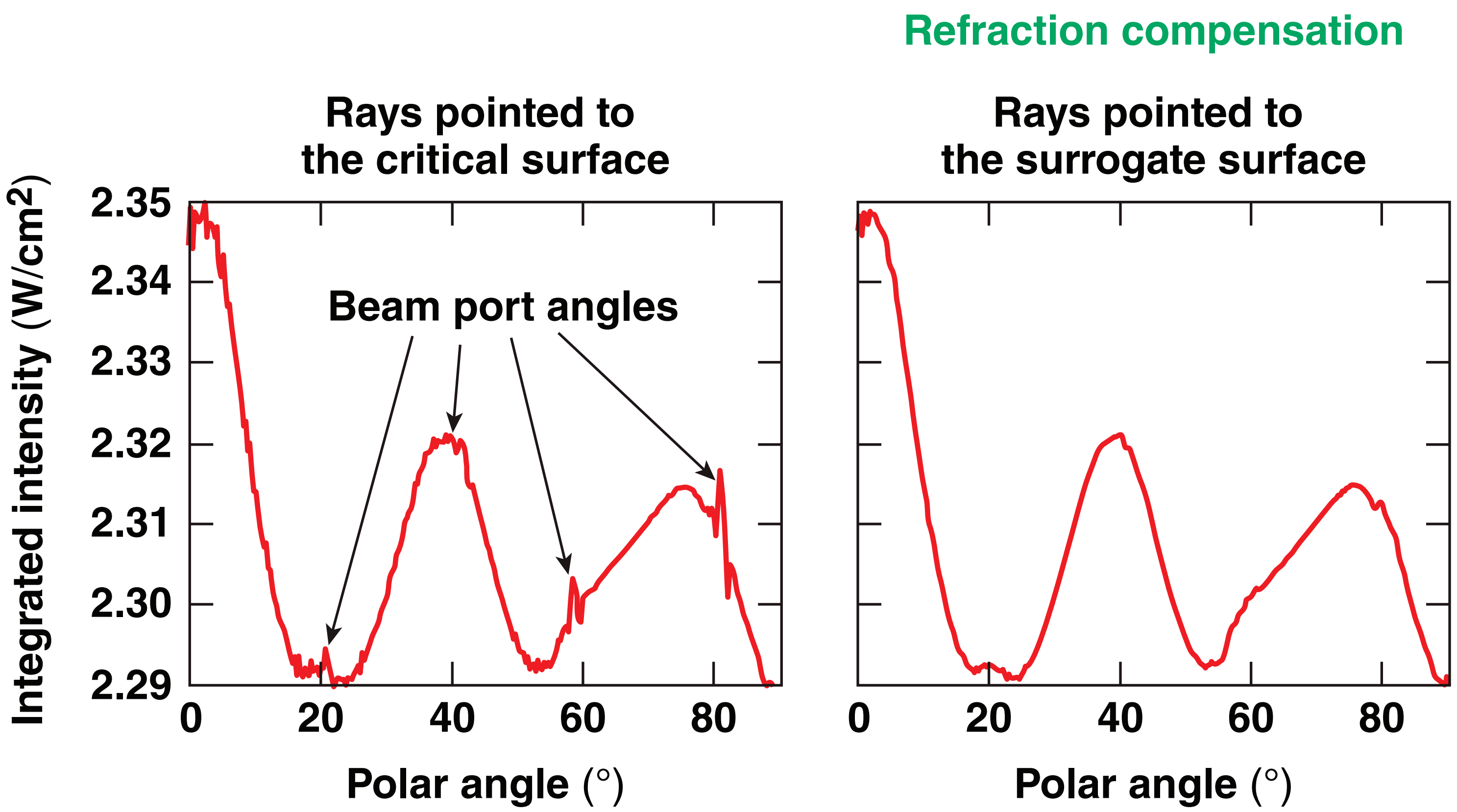


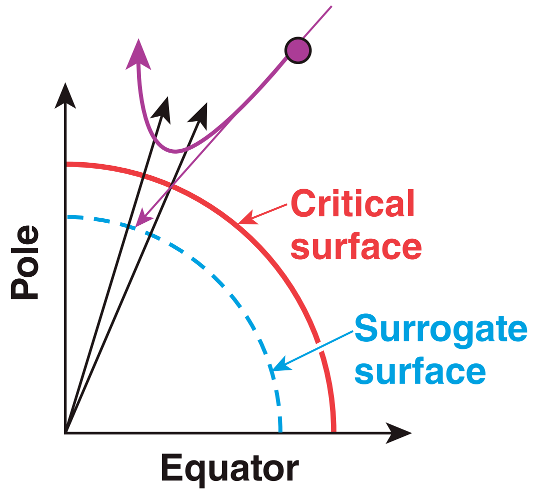


- An optimization algorithm locates the surrogate surface in *DRACO*
- *HYDRA* will employ this method plus a Delaunay/Voronoi triangulation method

TC14595

# A proof-of-principle approximation of the simple dynamic refraction compensation promises additional control of numeric noise in 3-D *HYDRA*

UR LLE

**OMEGA 60 beam**

- ~25M rays/ray-trace cycle
- End of pulse; $t \sim 2.5$ ns
- CR = 430/45 ~ 10

**Without compensation**

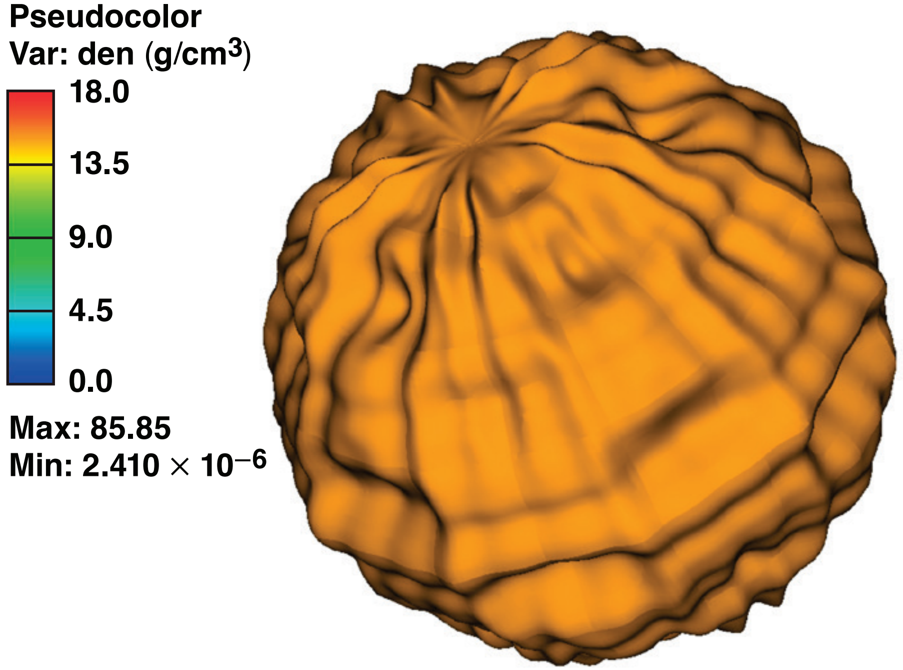


**With compensation**

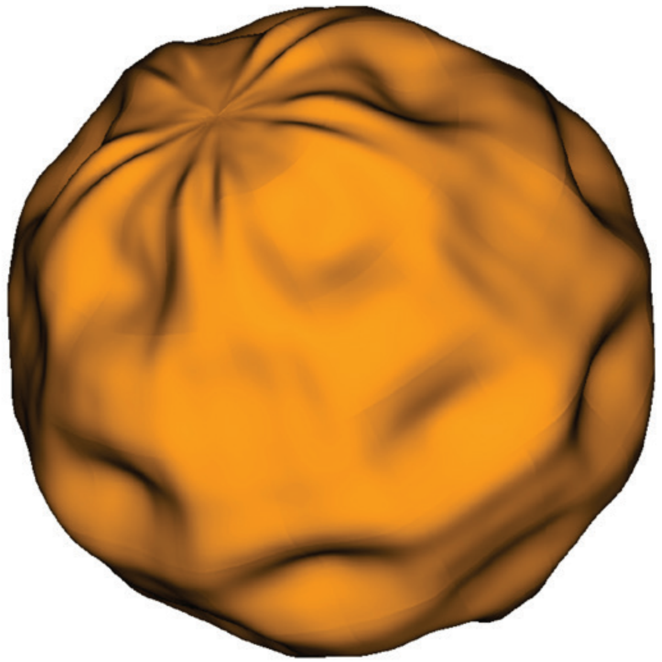

(15-g/cm$^3$ mass-density isosurface)

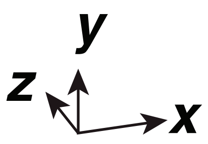


TC14596

# Radially integrated deposition patterns from *DRACO* illustrate the benefits of using adaptive integrators

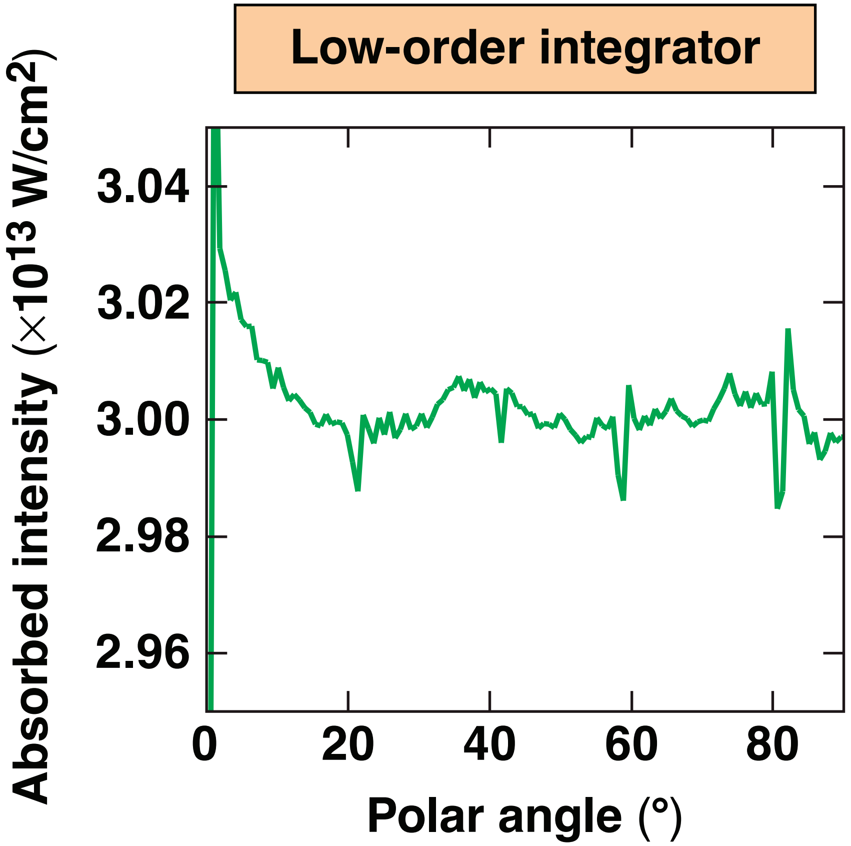


*t* ~ 450 ps

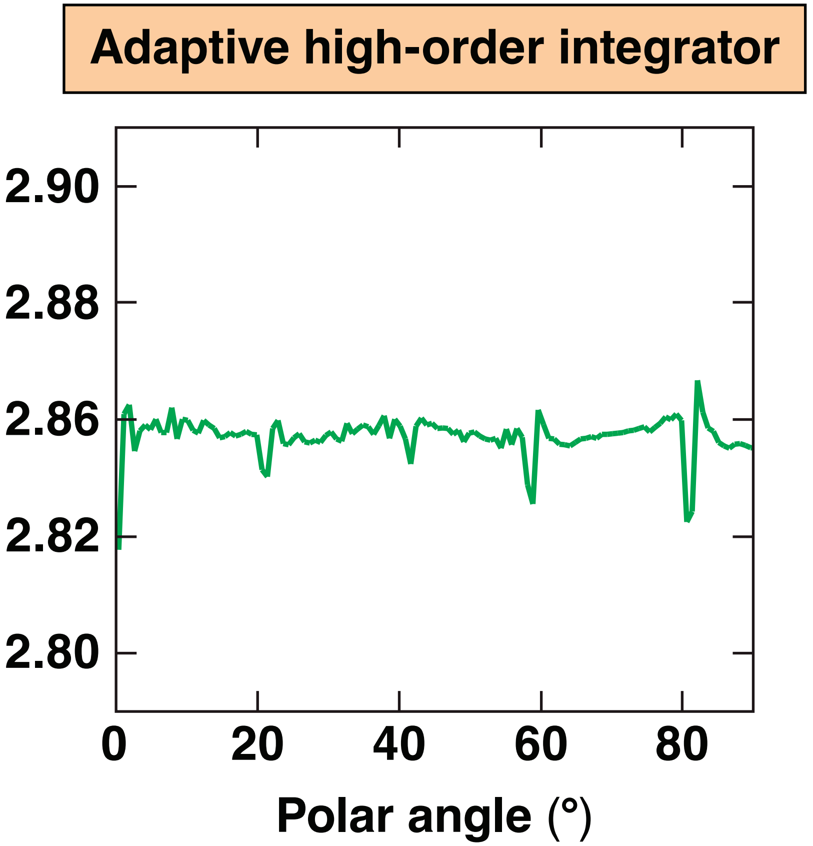


- Lower binning noise
- More accurate overall deposition
- Lower errors at beam centers
- More computationally efficient

TC14597

# Significant progress has been made implementing the LLE ray trace in *HYDRA*;* however, further work remains to minimize numerical noise

- The complete inverse projection method implemented in *DRACO*** offers many advantages that can port to *HYDRA*
  - low ray density achieves low noise levels; includes additional methods (below)
  - smooth deposition maximizes time steps → faster execution
  - the anticipated smooth deposition exposes potential noise sources
- The first stage of implementation is complete and significantly reduced noise levels to the order of the overlapped nonuniformity (~ few %)
- Additional methods are required for high-fidelity (noise below overlapped nonuniformity) direct-drive simulations
  - random dithering
  - dynamic refraction compensation (multiple methods)
  - adaptive ray integrators and cell-edge detection

**• Work on adapting the existing CBET model to direct drive in *HYDRA* will follow.**

*M. M. Marinak *et al.*, Phys. Plasmas 8, 2275 (2001).
**J. A. Marozas *et al.*, Phys. Plasmas 25, 056314 (2018).
M. M. Marinak *et al.*, UP11.00115, this conference.

# Backup slides

# The shell is more uniform using half the number of rays for inverse-projection, cf. the random distribution

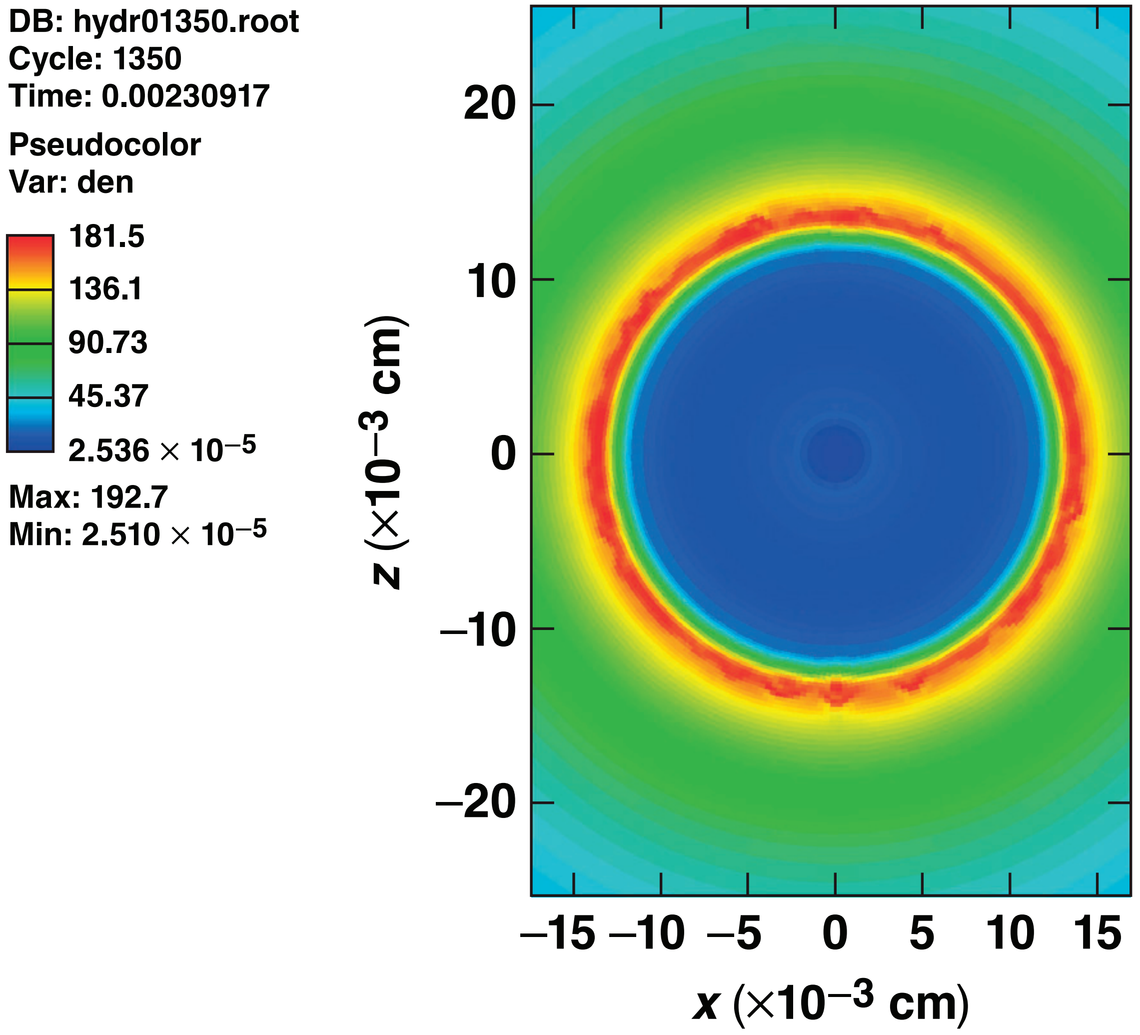


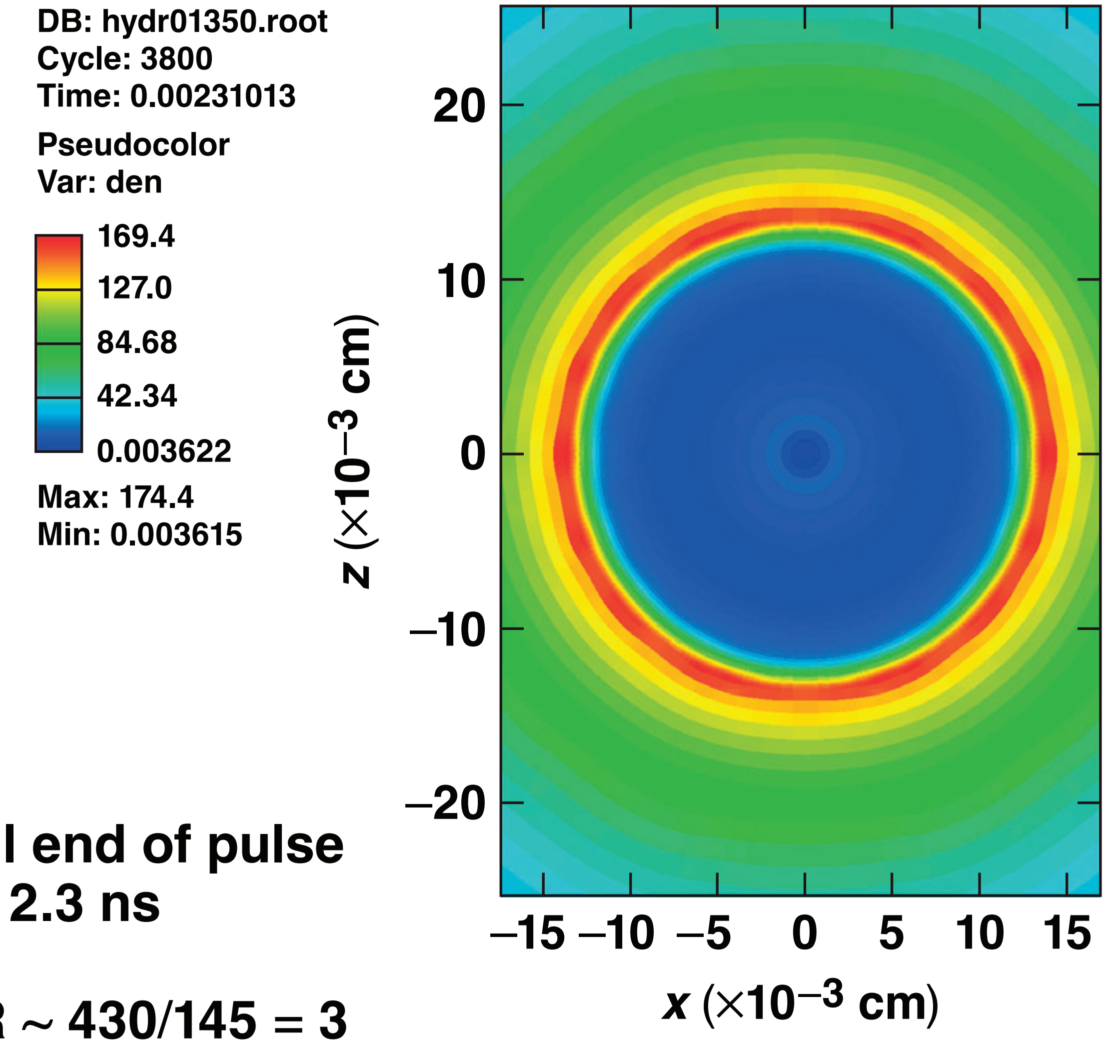


**Tail end of pulse**
**$t \sim 2.3$ ns**

**CR ~ 430/145 = 3**

TC14508

# Random dithering when combined with refraction compensation shows the most control of numeric noise in 3-D *HYDRA*



**With dithering**

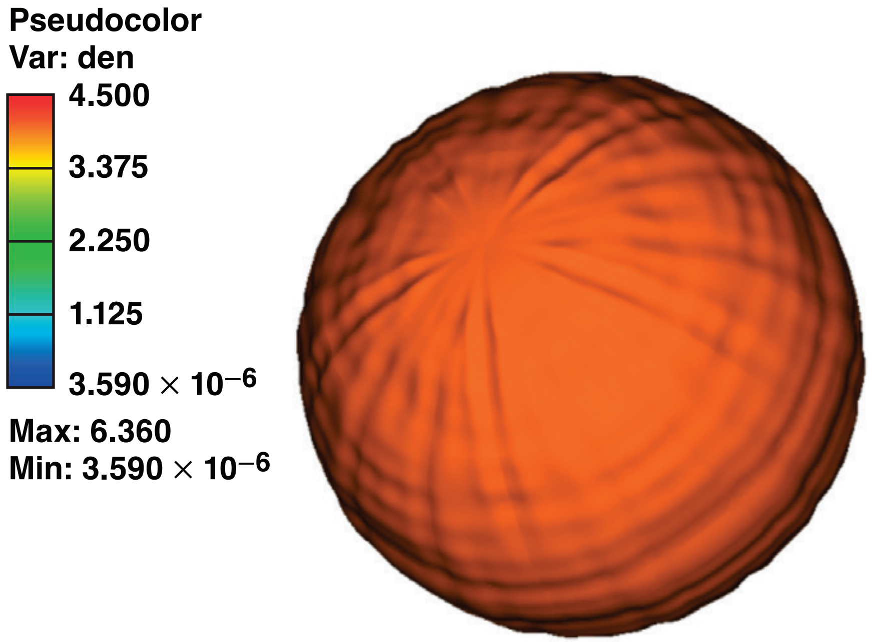


**Tail end of pulse**
***t*** **~ 2.3 ns**
**CR ~ 430/145 = 3**

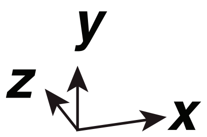


**With compensation and dithering**

TC14598